Surfactant effect of gallium during molecular-beam epitaxy of GaN on AlN (0001)

Guido Mula,[1,2] C. Adelmann,[1] S. Moehl,[1] J. Oullier,[1] and B. Daudin[1]

[1]*Commissariat à l'Energie Atomique, Département de Recherche Fondamentale sur la Matière Condensée, Service des Matériaux et Microstructures, 17 Rue des Martyrs, 38054 Grenoble Cedex 9, France*

[2]*Istituto Nazionale de Fisica della Materia and Dipartimento di Fisica, Università di Cagliari, Cittadella Universitaria, Strada Provinciale Monserrato–Sestu km 0.700, 09042 Monserrato (CA), Italy*

(Received 18 January 2001; revised manuscript received 29 June 2001; published 19 October 2001)

We study the adsorption of Ga on (0001) GaN surfaces by reflection high-energy electron diffraction. It is shown that a dynamically stable Ga bilayer can be formed on the GaN surface for appropriate Ga fluxes and substrate temperatures. The influence of the presence of this Ga film on the growth mode of GaN on AlN(0001) by plasma-assisted molecular-beam epitaxy is studied. It is demonstrated that under nearly stoichiometric and N-rich conditions, the GaN layer relaxes elastically during the first stages of epitaxy. At high temperatures the growth follows a Stranski-Krastanov mode, whereas at lower temperatures kinetically formed flat platelets are observed. Under Ga-rich conditions—where a Ga bilayer is rapidly formed due to excess Ga accumulating on the surface—the growth follows a Frank-van der Merwe layer-by-layer mode at any growth temperature and no initial elastic relaxation occurs. Hence, it is concluded that excess Ga acts as a surfactant, effectively suppressing both Stranski-Krastanov islanding and platelet formation. It is further demonstrated that the Stranski-Krastanov transition is in competition with elastic relaxation by platelets, and it is only observed when relaxation by platelets is inefficient. As a result, a growth mode phase diagram is outlined for the growth of GaN on AlN(0001).

DOI: 10.1103/PhysRevB.64.195406 PACS number(s): 81.15.Hi, 68.35.−p, 81.07.Ta, 68.55.Ac

I. INTRODUCTION

In the recent past, important efforts have been devoted to controlling the epitaxial growth mode of strained semiconductor layers. High performance of strained layer-based optoelectronic devices is closely related to the achievement of smooth and abrupt interfaces. On the other hand, island formation of the lower band-gap material can lead to strong zero-dimensional exciton localization, i.e., to the formation of quantum dots. The growth of quantum dots is particularly appealing when the surrounding crystal matrix contains a large number of structural defects that act as nonradiative recombination centers. This is the case of III-V nitrides that exhibit typical threading dislocation densities in the range of 10^8–10^{11} cm^{-2}.

A widely used method to grow defect-free self-assembled nanometric islands is the Stranski-Krastanov (SK) growth mode.[1] This technique has allowed for the growth of quantum dots using, e.g., InAs/GaAs,[2,3] Ge/Si,[4,5] and GaN/AlN (Refs. 6–8) heterostructures.

However, it is often desirable to be able to select the growth mode of a strained epitaxial layer, i.e., to choose whether quantum wells or quantum dots will be grown. A possible method is the use of a surfactant[9] in order to prevent from islanding and promote a two-dimensional (2D) growth mode up to the onset of plastic relaxation by introduction of misfit dislocations.

In the present paper, we study the Ga adsorption on (0001) GaN surfaces. We show by reflection high-energy electron diffraction (RHEED) measurements that a continuous Ga bilayer is formed on the GaN surface. It is further demonstrated that this film has a substantial influence on the initial elastic relaxation of (0001) GaN layers grown on AlN (2.4% lattice mismatch). As previously reported, initial strain relaxation occurs by elastic relaxation due to the formation of three-dimensional (3D) pyramidal GaN islands by a SK growth mode at high temperatures[6,7] or flat GaN platelets at low temperature.[10] However, as we will show below, both types of islanding are suppressed by the presence of the Ga film. Hence, Ga may be regarded as an autosurfactant for GaN growth. As a consequence, this allows to choose the growth mode of GaN on AlN(0001), i.e., to grow either quantum wells with smooth interfaces or 3D islands with quantum dot properties.[11]

II. EXPERIMENTAL PROCEDURE

The samples have been grown in a MECA2000 molecular-beam epitaxy (MBE) chamber equipped with a radio frequency (rf) plasma source from Applied Epi and conventional effusion cells for Ga and Al evaporation. The pseudosubstrates used were 1.5 μm thick (0001) GaN layers grown by metal-organic chemical vapor deposition (MOCVD) on sapphire. For the adsorption measurements, the pseudosubstrates were overgrown by about 50 nm of GaN to prevent from a possible surface contamination layer. For the GaN relaxation measurements, the pseudosubstrates were overgrown by 0.5 μm thick fully relaxed AlN layers.

Real-time recording of the RHEED pattern has been used to monitor Ga adsorption and desorption as well as to measure the variation of the in-plane lattice parameter during the first stages of GaN epitaxy on AlN.

For adsorption measurements, the temporal variation of the specular RHEED intensity has been recorded. Prior to the exposition to the Ga flux, we have stabilized the GaN surface under a N flux to ensure the reproducibility of the starting surface.

 ©2001 The American Physical Society

For lattice parameter measurements, the distance of the (10) and ($\bar{1}0$) RHEED streaks in the $\langle 11\bar{2}0\rangle$ azimuth was determined by gaussian fits. The substrate temperature was measured by a thermocouple kept in mechanical contact to the backside of the molybdenum sample holder. To study the influence of the growth rate on GaN relaxation, experiments were performed at two different N fluxes: 0.50 sccm N_2 flow at 300 W rf power, leading to maximum growth rates of about 0.3 monolayers (ML) per second, and 0.20 sccm N_2 flow at 200 W rf power, leading to maximum growth rates around 0.15 ML/s. GaN surface morphologies have been determined by atomic-force microscopy (AFM).

III. Ga ADSORPTION AND DESORPTION ON GaN

In this section, we will discuss the adsorption of Ga on (0001) GaN surfaces. The main point of this section is the formation of a stable, about 2 ML thick, Ga film on the GaN surface.

A. Experiments and Results

The wetting of the (0001) GaN surface by Ga was studied as a function of the substrate temperature and of the Ga flux. The adsorption experiments consisted in exposing the GaN surface to a Ga flux while recording the specular spot intensity in the RHEED pattern. Conversely, the desorption (consumption) of Ga was studied by measuring the variation of the specular spot intensity after shuttering of the Ga flux and subsequent exposure of the surface to vacuum (N plasma).

The duration of the intensity of the RHEED specular spot pseudo-oscillatory transient (see Fig. 1), observed immediately after opening the Ga cell shutter, was found to depend on the Ga cell temperature T_{Ga}. After closing the Ga cell shutter and opening the N cell shutter, a new transient in the RHEED specular spot intensity is observed, whose shape is roughly symmetric to the adsorption transient, although with a shorter duration. For all experiments on Ga adsorption, Ga desorption under vacuum and Ga consumption under N, the transient duration was determined graphically, as shown in the inset of Fig. 1, so that the transient end is unambiguously defined. In Fig. 2, the inverse of the Ga adsorption pseudo-oscillatory transient time has been plotted as a function of the beam equivalent pressure of the Ga cell. A linear dependence is found for each substrate temperature. We can account for this result by calculating the amount d of Ga adsorbed on the GaN surface during the pseudo-oscillatory transient duration, which is given by $d = s_{\mathrm{Ga}}\Phi_{\mathrm{Ga}}t_{\mathrm{ads}}$, where s_{Ga} is the Ga/GaN sticking coefficient, Φ_{Ga} is the Ga flux, and t_{ads} is the pseudo-oscillatory transient duration. Assuming a flux-independent Ga/GaN sticking coefficient, the linear dependence observed in Fig. 2 demonstrates that the ratio s_{Ga}/d is constant.

In Fig. 3 we show, for a substrate temperature of $T_S = 730\,°\mathrm{C}$, the variation of the duration of the Ga desorption transient under vacuum t_{des} as a function of the Ga deposition time t_{ads}. The Ga cell temperature was $T_{\mathrm{Ga}} = 1040\,°\mathrm{C}$, and t_{ads} was varied from 2 to 90 s. This experiment shows that t_{des} increases with the Ga deposition time up to about $t_{\mathrm{ads}} = 7$ s before saturating. This indicates that, in the experimental conditions, exposing the GaN surface to Ga flux for more than 7 s has no effect on the amount of Ga deposited. In particular, we have observed that, when exposing the GaN surface to the Ga flux alone for more than 1 h, the Ga desorption-related transient was still observed immediately

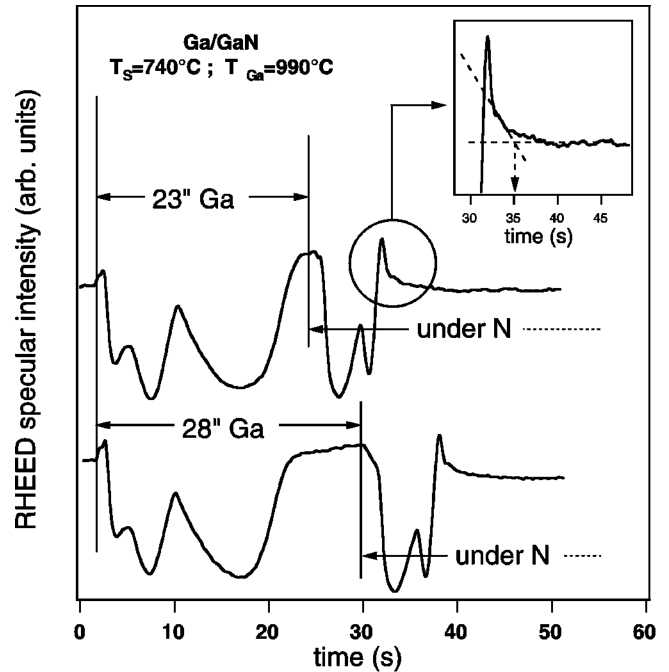

FIG. 1. Variation of the RHEED specular spot intensity as a function of time during exposure of the GaN surface to a Ga flux alone and subsequently to a N flux alone. The vertical lines correspond to the opening of the Ga cell shutter (left) and to the simultaneous closing of Ga cell shutter and opening of N cell shutter (right). Note that the Ga consumption transient is the same for the two curves corresponding to two different exposure times to Ga flux. The graphic method used for determining the transient end is shown in the inset.

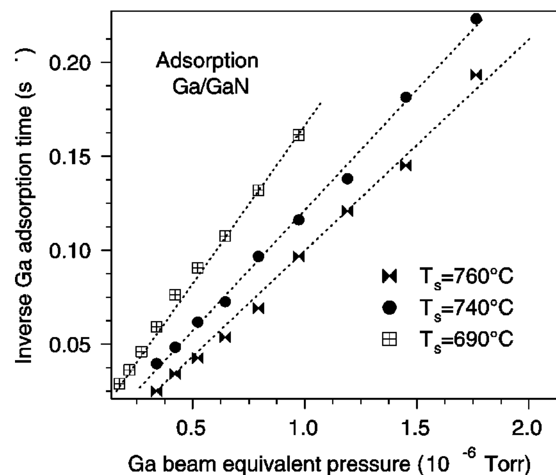

FIG. 2. Inverse of the Ga adsorption transient time on (0001) GaN as a function of the beam equivalent pressure of the Ga cell for $T_S = 690$, 740, and 760 °C.

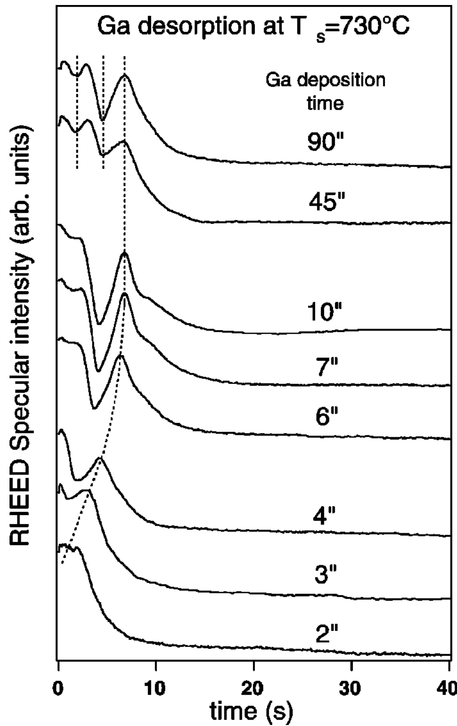

FIG. 3. Variation of the RHEED specular spot intensity during Ga desorption under vacuum as a function of time, after shuttering of the Ga cell. $T_S = 730°C$. The Ga deposition time was varied from 2 to 90 s. Note the saturation of the desorption time for deposition times longer than 7 s.

after the closing of the Ga cell shutter. Then, it is deduced that (dynamically) stable Ga films exist on GaN surfaces under conditions typically used in GaN MBE, i.e., Ga films of a definite thickness that does not vary with exposure time.

In another experiment, the deposited Ga was consumed by exposing the covered GaN surface to a N flux, identical to that we generally use for GaN growth (see Fig. 1). As mentioned above, the variation of the RHEED specular spot intensity recorded as a function of time first reveals that the recovery of the initial GaN surface occurs in an oscillatory mode, symmetric to the oscillations observed when exposing the GaN surface to Ga. This was verified for substrate temperatures in the $T_S = 700–750°C$ range. Similar to the case of Ga desorption under vacuum, a transient is observed immediately after the opening of the N cell shutter. This transient, related to the consumption of the adsorbed Ga under the N flux, also shows a saturation of its duration t_N as a function of t_{ads}. As shown in Fig. 1, the saturation of t_N indicates that above a critical t_{ads} no further Ga accumulation is observed.

We also exposed the GaN surface to much higher Ga fluxes (up to about four times higher), and we observed a t_{ads}-dependent delay between the closing of the Ga cell shutter and the beginning of the transients related to either Ga desorption or consumption under N that shows no saturation, i.e., no stable Ga films of finite thickness are observed. We interpret these results as a formation of Ga droplets on the surfaces. This was confirmed by optical microscopy of a sample exposed to such high Ga fluxes for 30 min.

It has to be noted that identical oscillatory transients due to the desorption of Ga have been observed after growing GaN in Ga-rich conditions. As for adsorption, dynamically stable conditions have been observed where the transient duration is independent of the previous growth time. This shows that excess Ga on a growing GaN surface behaves (at least qualitatively) like Ga adsorbed on a GaN surface without an impinging N flux. After GaN growth in Ga-rich conditions is initiated, excess Ga accumulates progressively on the GaN surface and finally forms a bilayer or, for very high Ga fluxes, Ga droplets.

B. Determination of the Ga film thickness

We will now determine quantitatively the amount of Ga contained in the continuous film deposited onto the GaN surface during the time span of the Ga adsorption-related transients. For this purpose, we will use the duration of both the transients related to, respectively, desorption under vacuum and consumption under N. The Ga consumption under N is then given by a first-order rate equation

$$\frac{d\rho}{dt} = -v_{\mathrm{GaN}} - \Phi_{\mathrm{des}}, \tag{1}$$

where ρ is the Ga adatom density, v_{GaN} the GaN growth rate under N-limited conditions, and Φ_{des} the Ga desorption rate under vacuum. The Ga desorption rate will generally be a function of the Ga adatom density, which may be nonlinear for multilayer adsorption. However, a first-order approximation can be obtained by assuming that $\phi_{\mathrm{des}} \cong \Gamma$ is constant. This approximation is at least valid in the limit of vacuum desorption rates that are small with respect to the GaN growth rates, which is the case for $T_S \leqslant 730°C$. In general, the approximation should lead to a slight overestimation of the Ga film thickness, provided that the real Ga desorption rate is a concave function of the Ga surface coverage. Using this approximation, we can calculate the amount d of Ga contained in the film as

$$d = \frac{v_{\mathrm{GaN}}}{(1/t_{\mathrm{N}} - 1/t_{\mathrm{des}})}, \tag{2}$$

where t_N is the duration of the transient for Ga consumption under N and $t_{des} = d/\Gamma$ is the duration of the transient for Ga desorption under vacuum.

In Fig. 4 we show the experimental curves obtained at $T_S = 720°C$, for (a) N-limited RHEED oscillations, (b) the RHEED transient associated to the desorption of the Ga film under vacuum, and (c) the RHEED transient associated to the consumption of the Ga film under N. By applying Eq. (2), we obtain a Ga film thickness of $d = 2.7$ ML (in units of GaN atomic surface density). We have repeated this measurement for several other T_S in the 700–740°C range, which modifies strongly the relative weight of the terms of Eq. (2). We found a good agreement of the measurements of the Ga film thickness obtained for all the T_S, within a ± 0.3 ML fluctuation, supporting that the Ga desorption process is correctly taken into account in our calculations. We

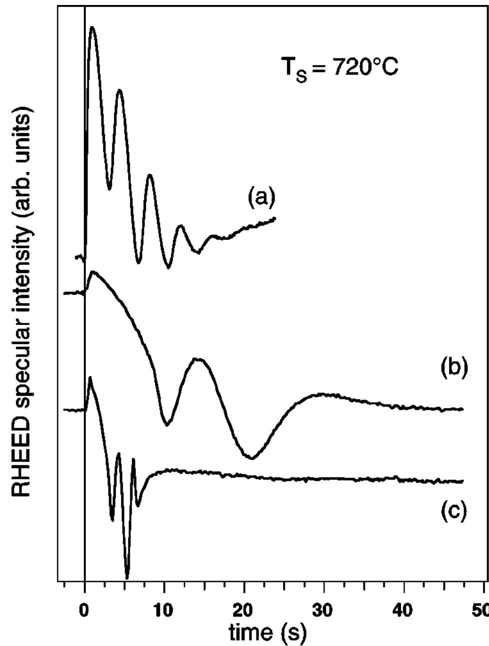

FIG. 4. (a) N-limited RHEED oscillations, (b) Ga vacuum desorption transient, (c) Ga consumption under N transient. The substrate temperature is 720°C in all cases. The exposure times to Ga flux were identical (90 s) for both vacuum desorption and N consumption of the Ga film.

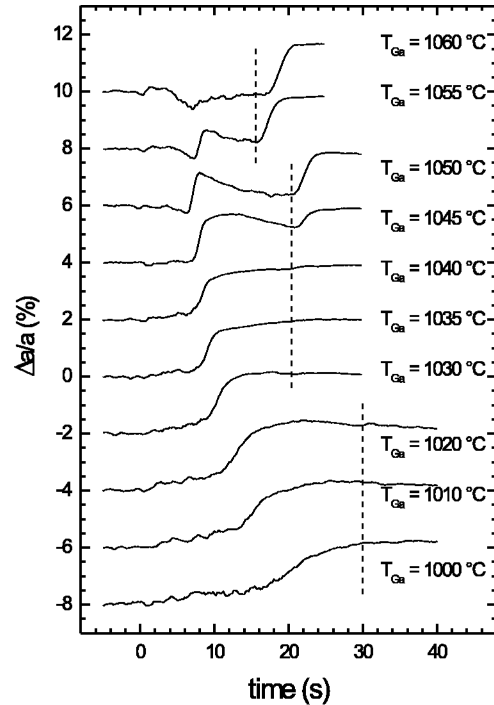

FIG. 5. Relative variation of the in-plane lattice parameter a during the growth of GaN on AlN. The substrate temperature was $T_S=740°C$, the N_2 flow 0.50 sccm at 300 W rf power, and the Ga cell temperature as indicated. The dashed lines indicate the growth interruption under N flux.

can then conclude that the thickness of the continuous Ga film deposited is about (2.7 ± 0.3) ML.

As stated above, the reciprocal duration of the adsorption transient is a linear function of the impinging Ga flux (see Fig. 2). This led us to the conclusion that the ratio s_{Ga}/d is constant. As also stated above, the Ga film thickness is the same within the experimental precision for all temperatures considered in the paper. Therefore, the decrease of the slopes in Fig. 2 reflects the decrease of the Ga sticking coefficient s_{Ga}.

It has to be stressed that the relation between the amount of Ga necessary to saturate the GaN surface and the actual thickness of the Ga film is far from being obvious, since it depends on the surface atomic density of the Ga film with respect to the GaN surface atomic density. Concerning the surface atomic density of the Ga film, the Ga bilayer model of Northrup *et al.*[12] predicts that the first monolayer, being matched to GaN, exhibits the same atomic surface density than GaN. The second monolayer should be instead laterally contracted and exhibit a surface atomic density about 30% higher. As a consequence, the bilayer is expected to contain $1+1.3=2.3$ ML of Ga, in terms of GaN atomic surface density. This compares rather favorably to our result taking into account the fact that our model tends to overestimate the amount of Ga contained in the film.

IV. RELAXATION OF GaN ON AlN

As discussed in the previous section, Ga forms a bilayer on the (0001) GaN surface during growth in Ga-rich conditions. One might then wonder whether the presence of such a continuous Ga film changes the GaN growth kinetics and relaxation mechanism or not. In this section, we will examine the inital relaxation of GaN layers grown on (0001) AlN as a function of the III/V ratio and the substrate temperature.

A. High-temperature regime: Stranski-Krastanov growth

Figure 5 shows the relative temporal variation of the in-plane lattice parameter $\Delta a/a$ for different Ga fluxes at a substrate temperature of $T_S=740°C$. The N_2 flow was 0.50 sccm at 300 W rf power, the growth rates were at maximum around 0.3 ML/s.

Let us start the analysis with a Ga effusion cell temperature of $T_{Ga}=1040°C$. Under this condition, the GaN growth is nearly stoichiometric. Initially, the in-plane lattice parameter shows almost no variation, followed by a rapid increase after 8 s of GaN deposition. The apparent relaxation after 8 s, corresponding to the deposition of approximately 2 ML, has been previously explained in terms of elastic relaxation by GaN islanding.[6] Together with the formation of a strained wetting layer during the first 8 s, this behavior is characteristic of the Stranski-Krastanov growth mode. The resulting islands have been characterized by RHEED, AFM [see Fig. 6(a)], and transmission electron microscopy. They have been found to be truncated hexagonal pyramids with $\{10\bar{1}3\}$ facets, typical diameters of 15 nm, typical heights of 3 nm, and an aspect ratio of about 1/5.[7]

For lower Ga fluxes, i.e., for increasingly N-rich growth, the phenomenology remains essentially the same. The

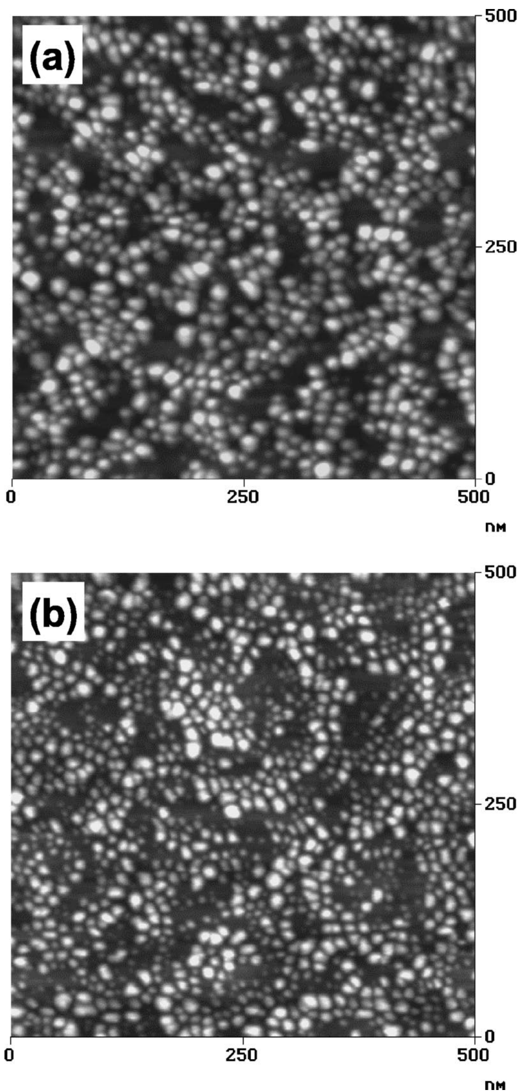

FIG. 6. Atomic-force micrographs of (a) GaN islands, grown in the Stranski-Krastanov mode and (b) GaN islands formed during a growth interruption under N after Ga-rich GaN growth. $T_S = 730°C$ in both cases. The island densities are 2.7×10^{11} cm^{-2} and 4.0×10^{11} cm^{-2}, respectively. The z-scales are 8 nm for both images.

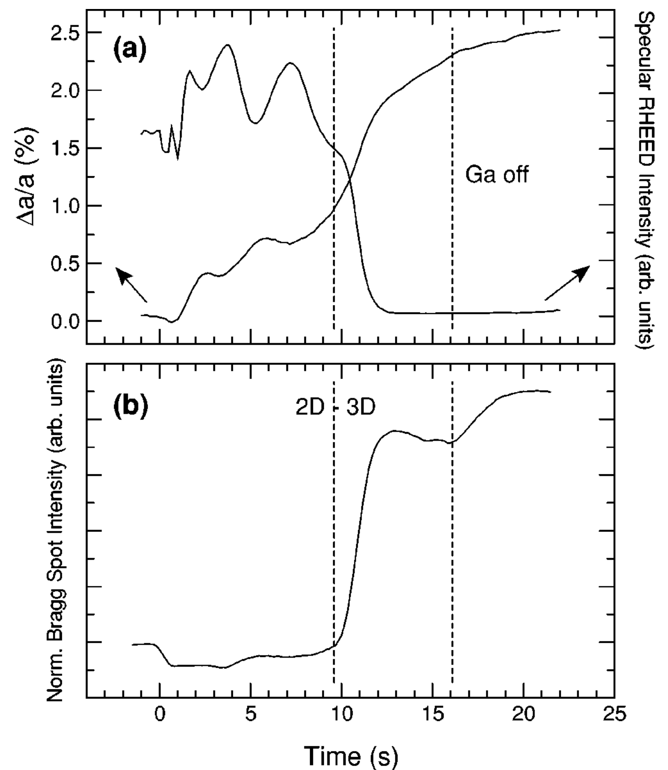

FIG. 7. Variation of the in-plane lattice parameter, the RHEED specular spot intensity, and the $(10\bar{1}2)$ Bragg spot intensity during the growth of GaN on AlN under moderately N rich conditions. The Bragg spot intensity has been normalized with respect to the overall intensity of the RHEED pattern. The substrate temperature was $T_S = 740°C$, the N_2 flow 0.50 sccm at 300 W rf power.

2D–3D transition becomes smoother as the GaN growth rate decreases for lower Ga flux. Note that below $T_{Ga} = 1030°C$ a small lattice parameter relaxation is observed during wetting layer deposition, that we assign to a weak surface roughening due to N-rich growth[13] associated with the emergence of very flat 2D platelets, maybe 1–2 ML high.[14]

The existence of such 2D platelets on the wetting layer is evidenced in Fig. 7. Here we show the relative variation of the in-plane lattice parameter and the variation of the RHEED specular spot and the $(10\bar{1}2)$ Bragg spot during the growth of another GaN layer on AlN at $T_S = 740°C$ under moderately N-rich conditions (equivalent to $T_{Ga} \approx 1020–1030°C$). While the Bragg spot intensity remains constant during the first 10 s [Fig. 7(b)], i.e., the surface morphology remains quasi-2D, we observe oscillations in both the RHEED specularly reflected intensity and the lattice parameter [Fig. 7(a)].[15] These oscillations are a marker of layer-by-layer growth. However, the in-plane lattice parameter does not return to its fully strained value after the first oscillation, suggesting that a second layer is nucleated before the first is completed. As a consequence, 1–2 ML high 2D platelets, that relax elastically at their borders, are found on the surface. After 10 s we see an abrupt rise both in the Bragg spot intensity and in the lattice parameter, which indicates the 2D–3D transition, i.e., the formation of GaN pyramids. In parallel, the reflected RHEED intensity decreases strongly due to islanding.

Let us come back to Fig. 5. If the Ga flux is increased above $T_{Ga} = 1040°C$, the growth conditions become Ga-rich and a Ga bilayer is progressively formed by excess Ga. A feature that attracts the attention is that at high Ga fluxes ($T_{Ga} = 1060°C$), no relaxation of the in-plane lattice parameter is observed, i.e., no 2D–3D transition and thus no formation of GaN pyramids during growth. The small transitory drop observed in $\Delta a/a$ after about 10 s of GaN growth has also been observed for Ga adsorption on GaN surfaces and may be thus related to the Ga bilayer formation. Albeit its orgin is not yet clear, it may be due to stress induced by the Ga bilayer or reflect the smaller mean lattice parameter of the Ga overlayer.[12]

For intermediate Ga fluxes, an initial relaxation is observed after a 2D–3D transition, followed by a decrease of the lattice parameter, i.e., the GaN layer becomes more

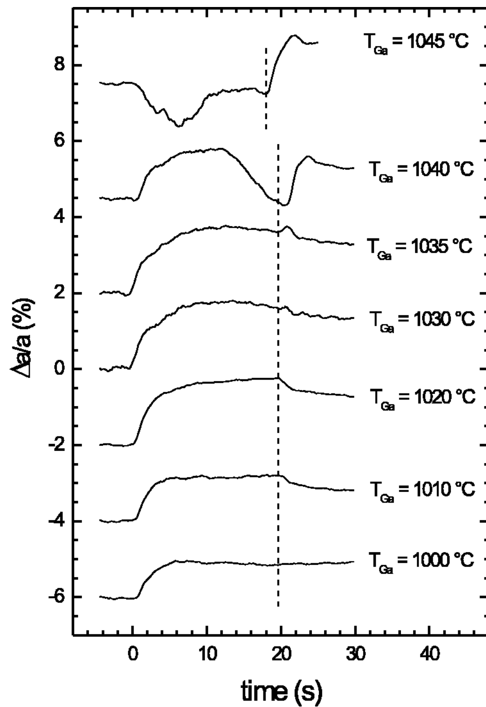

FIG. 8. Relative variation of the in-plane lattice parameter a during the growth of GaN on AlN. The substrate temperature was $T_S = 660°C$, the N_2 flow 0.50 sccm at 300 W rf power, and the Ga cell temperature as indicated. The dashed lines indicate the growth interruption under N flux.

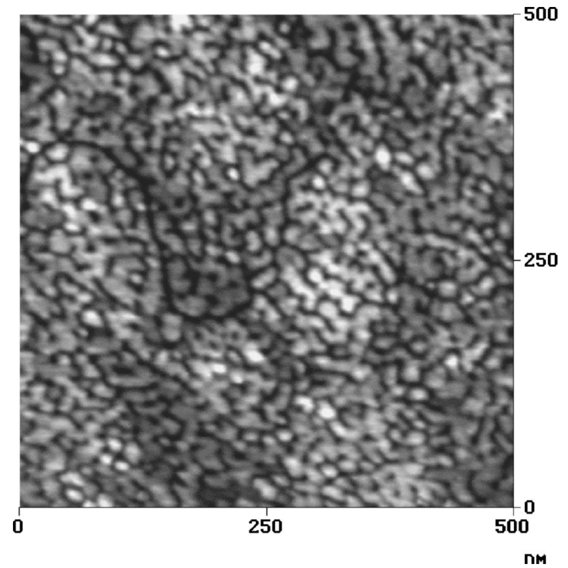

FIG. 9. Atomic-force micrograph of GaN platelets formed during growth interruption under N after Ga-rich GaN growth on AlN. $T_S = 640°C$. The z-scale is 4 nm.

strained. Thus, we observe a transitory formation of GaN pyramids followed by islands coalescence and the formation of a smooth growth front. This reversibility also unambiguously demonstrates that the relaxation is elastic.

After depositing 4–5 ML of GaN, the Ga flux has been interrupted and the surface kept under N flux alone. For near-stoichiometric and N-rich conditions, no significant variation of the in-plane lattice-parameter is observed. It has been shown that a ripening effect occurs under N flux, although much weaker under N than under vacuum.[7]

As discussed above, under Ga-rich growth conditions no GaN pyramids are formed or they coalesce quickly. An interesting feature is that a 2D–3D transition is again observed under N flux, as indicated by a rapid increase in the in-plane lattice parameter. The RHEED pattern shows the same $\{10\bar{1}3\}$ facets observed for the pyramids formed during growth at lower Ga fluxes. AFM reveals islands with typical diameters of 15 nm and typical heights of 3 nm [Fig. 6(b)]. This leads to an aspect ratio of 1/5, identical to that of the pyramids obtained during growth at lower Ga fluxes. As a result, we can conclude that the islands formed under N flux are indistinguishable from those formed during growth.

B. Low-temperature regime: Platelet formation

The situation is quite different for lower substrate temperatures. Figure 8 shows the relative variation of the in-plane lattice parameter obtained for a substrate temperature of $T_S = 660°C$ at a N_2 flow of 0.50 sccm at 300 W rf power, i.e., for maximum growth rates around 0.3 ML/s.

Let us start the analysis again with near-stoichiometric conditions at a Ga effusion cell temperature of $T_{Ga} = 1030°C$. In contrast to the high-temperature results described above, we observe a significant increase of the in-plane lattice parameter from the very beginning of the growth. This behavior is distinctly different from that of the SK growth mode because of the lack of a 2D wetting layer. The effect has been observed previously and attributed to the formation of GaN platelets that relax elastically at their borders.[10] These platelets have been found to be flat islands with heights of around 4 ML (1 nm) and diameters of around 15 nm (see Fig. 9). The aspect ratio of the platelets is thus about 1/15, which is to be compared to the value of 1/5 for the pyramidal-shaped SK islands obtained at higher temperatures.

As mentioned above, such an immediate elastic relaxation of the wetting layer is also observed at higher temperatures, at least under strongly N rich conditions. However, the relaxation is found to be much weaker. Hence, the platelets formed at higher temperature have a lower aspect ratio, as the relaxation yield is, in first approximation, proportional to the aspect ratio of the platelet.[10,16] Also the platelets' heights may be lower.

For lower Ga fluxes (N-rich growth), no qualitative difference is found. The maximum relaxation due to platelets is lesser, maybe due to smaller islands at a higher density. However, similar to the high-temperature case, no relaxation of the GaN epilayer is observed for Ga-rich conditions ($T_{Ga} \geq 1045°C$) and the epilayer remains fully strained. The drop in the in-plane lattice parameter at the beginning of the growth is observed again, maybe related to the Ga excess film. Once more, for slightly Ga-rich growth, a transitory relaxation is found, followed by a decrease of the in-plane lattice parameter, in full accordance with the results in Ref. 10.

During growth interruption under N flux, no effect is found for near-stoichiometric or N-rich conditions. Similar to high-temperature case, again relaxation occurs for growth interruptions under N when the growth has previously been carried out under Ga-rich conditions (see Fig. 8, $T_{Ga} \geqslant 1040°C$), i.e., again platelets are formed by consuming the excess Ga available on the surface (see Fig. 9).

V. DISCUSSION

A. Stranski-Krastanov growth and Ga surfactant effect

At a first glance, the observed suppression of the 2D–3D transition under Ga excess conditions seems analogous to the case of InAs grown on GaAs (Ref. 17) or on InP (Ref. 18), where the 2D–3D transition is also inhibited by metal-rich, i.e., In-rich, growth conditions. This effect has been explained by the fact that the surface free energy and the step formation free energy of In-rich 4×2 reconstructed InAs surfaces is higher than that of As-rich 2×1 reconstructed surfaces.[17,18] A higher surface free energy increases the energetic cost of free surface creation and should thus hamper islanding. Similarly, it has been also observed that a high AsH_3 partial pressure in the MOCVD growth of InGaAs on GaAs postpones the 2D–3D transition, which has also been assigned to an increase in surface free energy.[19]

However, in the case of GaN, the observed surface structures and reconstructions are essentially different: as we have shown above, the structure of the pseudo-1×1 GaN (0001) Ga-rich surface—generally encountered under Ga-rich MBE conditions—consists of an adsorbed Ga bilayer on top of the Ga terminated GaN surface, in agreement with previous theoretical[12,20] and experimental[20] results. In fact, the calculations show that the surface free energy of the Ga-rich pseudo-1×1 surface is lower than that of the N-rich 2×2 reconstructed surface.[12] Although no calculations have yet been performed for the $\{10\bar{1}3\}$ facets of the pyramids, we speculate that the effect of the Ga bilayer will be similar. Hence, from that point of view, Ga pyramid formation should even be fostered under Ga-rich conditions.

Another way to suppress island formation is the use of surfactants.[9,21] The role of a surfactant is to promote wetting of the substrate by the epilayer and thus avoid islanding. Furthermore, the surfactant has a strong tendency to segregate and float on the growing surface without being incorporated. Such a surfactant effect has been observed for, e.g., As and Sb in the Ge/Si system[9,21–23] as well as Te in the InAs/GaAs and InGaAs/GaAs systems.[24,25] Surfactants have also been observed in metal epitaxy.[26,27] For both Ge/Si and InAs/GaAs, the 2D–3D transition in the SK growth mode is suppressed by the presence of an adsorbed surfactant layer and the growth follows a Frank-van der Merwe growth mode. Finally, the Ge or InAs epilayer will relax plastically by emission of misfit dislocations.[25,28]

Concerning microscopic processes of surfactant-mediated growth, Copel *et al.*[21] proposed two possible mechanisms for surfactant action: the first is a kinetic mechanism by enhanced incorporation of the growth species and, as a consequence, reduced diffusion. The second is a static mechanism based on the modification of the surface strain due to the adsorbed surfactant layer. Alternatively, a kinetic model has been proposed by Kandel and Kaxiras.[29] It explains the suppression of 3D islanding by a passivation of step edges by surfactant atoms. As a consequence, incorporation at steps is hindered and 2D island nucleation is enhanced.

The first mechanism has been proposed to be active in the case of As and Sb in the Ge/Si (Refs. 30–32) and Te in the InAs/GaAs (Refs. 33–37) systems: the lower free energy of surfactant-terminated surfaces provides a strong driving force to an exchange of Ge or Si adatoms with surfactant atoms. The Ge or Si atoms are thus rapidly incorporated in subsurface sites and will nucleate as small 2D islands. Hence, the density of freely diffusing Ge or Si atoms adsorbed on top of the surfactant layer is low, preventing from nucleating large 3D islands.

However, in the case of GaN, this impediment to diffusion should be absent. Here, the candidate for rapid exchange with the floating Ga layer would be a N adatom. In fact, the exchange should be actually effective since the surface free energy of the Ga-rich pseudo-1×1 surface is lower than that of the 2×2 N-rich surface, as discussed above. However, it has been calculated for the case of an adsorbed In bilayer on GaN that subsurface diffusion of N atoms between the two In layers is extremely effective, more effective than, e.g., on N-rich surfaces.[38,39] An analogous behavior can also be expected for an adsorbed Ga layer.[39] As a consequence, such a mechanism by diffusion impediment should be discarded.

It is difficult to discuss the validity of the model of Kandel and Kaxiras,[29] since kinetic parameters and the step edge energetics for Ga-rich GaN growth are still scarcely known. In contrast, we will address the influence of the adsorbed Ga bilayer on the elastic properties of the surface. As discussed in Ref. 12, the first of the two absorbed Ga layers is expected to be coherent to the GaN layer beneath. This Ga layer should be under large tensile strain, since the equilibrium lattice parameter of Ga is about 15% smaller than that of GaN.[12] In the case considered here, the GaN layer and the Ga adsorbate are coherent to the AlN substrate. Then, the GaN layer is compressively strained by $\epsilon=2.4\%$ and the adsorbed Ga layer is tensilely strained by $\epsilon\approx12.5\%$. As a consequence, the relaxation of a compressively strained GaN layer on AlN should lead to further increasing the tensile strain of the Ga layer. In other words, the energy gain by GaN relaxation may be (partially) balanced by the increase in elastic energy of the Ga layer.

This point was further examined by growing GaN pyramids in a SK mode at $T_S=740°C$ and subsequently exposing them to a Ga flux. The corresponding variation of the in-plane lattice parameter is shown in Fig. 10. Initially, one observes the elastic relaxation of the GaN pyramids formed after about 8 s. However, after the pyramids have been exposed to Ga flux, the lattice parameter decreases by 0.7%, i.e., the GaN layer is partially restrained by the adsorbed Ga layer, as an evidence of a partial reversibility of the 2D–3D transition.

These features support the idea that the observed inhibition of the 2D–3D transition in the case of GaN growth in Ga-rich conditions is due to the surface stress applied by the

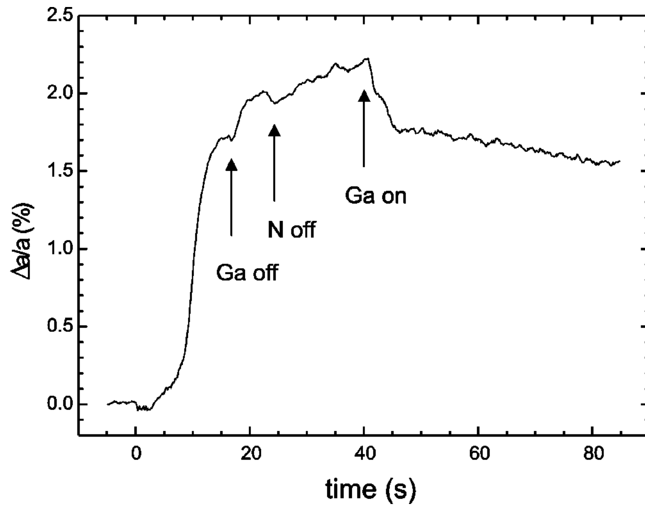

FIG. 10. Relative variation of the in-plane lattice parameter *a* during the growth of GaN pyramids on AlN, subsequently exposed to a Ga flux. $T_S = 740\,°\mathrm{C}$.

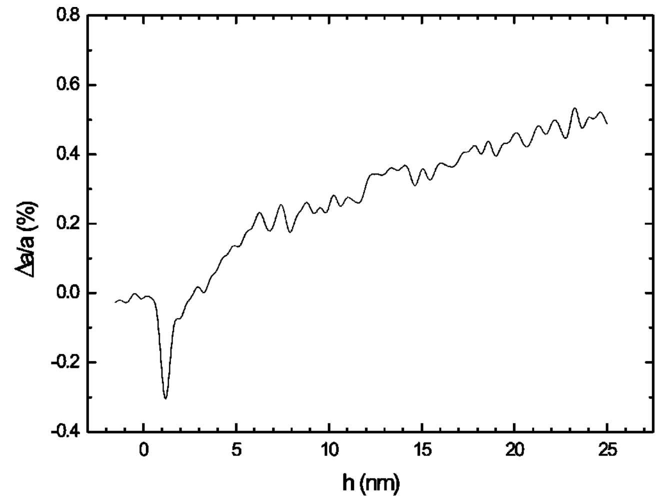

FIG. 11. Relative variation of the in-plane lattice parameter *a* during the growth of GaN on AlN under Ga-rich conditions. $T_S = 720\,°\mathrm{C}$, $T_{\mathrm{Ga}} = 1060\,°\mathrm{C}$.

Ga adsorbate. Furthermore, partial reversibility of GaN islanding during growth is also observed under moderately Ga-rich conditions ($T_{\mathrm{Ga}} = 1045-1055\,°\mathrm{C}$). As discussed in the previous section, pyramids are initially formed after a critical wetting layer thickness of about 2 ML. Thereafter, the islands transform again into a strained GaN film. This transitory is due to the fact that building up the adsorbed Ga layer takes a finite time for finite Ga excess. If this time is larger than that at which the 2D–3D transition takes place, islanding occurs first, becoming unfavorable after the Ga adsorbate layer is completed. This leads to a change in the surface morphology and the GaN film becomes almost pseudomorphic again. Under strongly Ga-rich conditions, the adsorbed Ga layer is almost immediately formed (i.e., faster than the time required for achieving the critical GaN layer thickness) and thus islanding never takes place.

We remark that a somehow similar effect of reversible islanding has been observed by exposing InGaAs islands on GaAs to a PH_3 flux.[40] This effect is explained by P atoms being substituted to As atoms in InGaAs islands. The lower mismatch of the resulting InGaAsP layer with respect to the GaAs substrate removes the thermodynamic driving force of islanding and the surface becomes flat. Of course, no atom substitution will occur for Ga on GaN. However, as in the above case, it is the elastic energy that is responsible for the observed 3D–2D morphology transformation.

When the Ga flux is interrupted, and the surface is kept under N flux alone, the Ga film present at the surface is consumed and contributes to further GaN growth. This also implies that its contribution to the elastic energy of the system vanishes. Since the growth has been carried out beyond the critical thickness of 2 ML, the GaN epilayer finds itself in strong nonequilibrium. Hence, the initially completely strained layer relaxes again by the formation of pyramids. As a result, we observe a 2D–3D transition under N flux, as shown above. However, since it is difficult to assess precisely the Ga excess, it is not yet clear if the pyramids are formed only by consuming the floating Ga or by a reorganization of the GaN layer.

When no growth interruption under N is performed, the RHEED pattern remains streaky under Ga-rich conditions even for thick GaN layers. The relaxation will be plastic and dislocations will be emitted gradually at higher GaN layer thickness (see Fig. 11).

B. Elastic relaxation by platelets

As in the case of SK pyramids, a critical Ga flux exists also for platelets (Fig. 8), above which the platelets are not stable and either coalescence of platelets soon after their formation or direct 2D growth alone is observed. For $T_{\mathrm{Ga}} = 1030\,°\mathrm{C}$ coalescence just begins on the experiment time scale, but if we increase T_{Ga} up to $1040\,°\mathrm{C}$ we observe a decrease of the lattice parameter to the value of relaxed AlN, indicating that the GaN layer is fully strained.

This shows that the surfactant effect of Ga is also effective to suppress the formation of GaN platelets at lower growth temperatures. Hence, the above discussion for quantum dots can also be applied to these observations. However, platelet formation seems to be rather due to surface kinetics and limited adatom diffusion at low temperatures than to thermodynamics, as for the SK case. It has been calculated that Ga and N adatom diffusion is greatly enhanced on Ga-stable surfaces with respect to N-stable surfaces.[41] At high adatom diffusion mobility, second layer nucleation is expected to be suppressed and the growth occurs in a layer-by-layer or step flow growth mode.[42] Thus, the finding that the relaxation by platelets becomes larger with decreasing substrate temperature and increasing N excess strongly corroborates the idea of growth kinetics being responsible for platelet formation.

In the case of heteroepitaxial growth of GaN on AlN, actually both effects—diffusion enhancement and surface strain modification—may collaborate to suppress platelet formation. Conversely, concerning the SK growth mode at higher temperature, enhanced diffusion should however promote pyramid formation. As a matter of fact, it has been shown that reduced diffusion at low growth temperature can

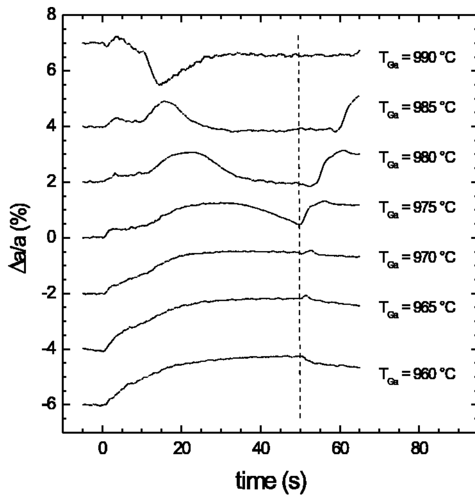

FIG. 12. Relative variation of the in-plane lattice parameter a during the growth of GaN on AlN. The substrate temperature was $T_S = 660°\text{C}$, the N_2 flow 0.20 sccm at 200 W rf power, and the Ga cell temperature as indicated. The dashed lines indicate the growth interruption under N flux.

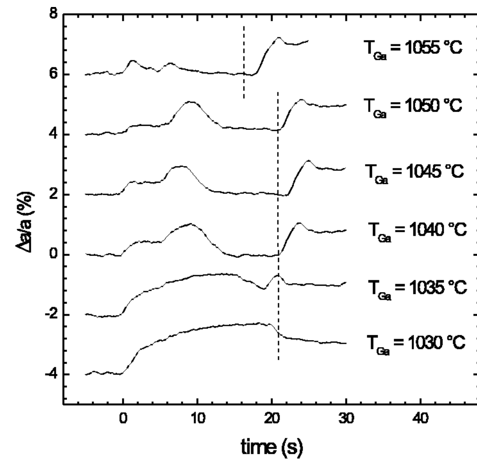

FIG. 13. Relative variation of the in-plane lattice parameter a during the growth of GaN on AlN. The substrate temperature was $T_S = 680°\text{C}$, the N_2 flow 0.50 sccm at 300 W rf power, and the Ga cell temperature as indicated. The dashed lines indicate the growth interruption under N flux.

be used to suppress the SK transition in the InAs/GaAs system.[43] We also recall that one of the proposed mechanisms for the surfactant effect of As on the growth of Ge on Si is the reduction of the effective Ge adatom diffusion length.[30–32]

C. Influence of platelets on Stranski-Krastanov growth

In Fig. 12 we show a set of lattice parameter variation curves obtained at $T_S = 660°\text{C}$ for a N_2 flow of 0.20 sccm at 200 W rf power (maximum growth rates around 0.15 ML/s). As a whole, the behavior is similar to that observed at higher growth rates: platelet formation is found for N-rich conditions and pseudomorphic growth for Ga-rich conditions. However, in this case, under moderately Ga-rich conditions, i.e., for $T_{\text{Ga}} < 990°\text{C}$, we observed a clear slope change in the lattice parameter variation after about 10 s of growth (≈ 1.5 ML) for $T_{\text{Ga}} = 970–985°\text{C}$. This variation can be explained by a morphology transition from flat platelets to larger islands with a higher aspect ratio after 1.5 ML of GaN. The same effect is found for higher growth rates (N_2 flow 0.50 sccm at 300 W rf power, maximum growth rates around 0.3 ML/s) at a substrate temperature of $T_S = 680°\text{C}$ (see Fig. 13, $T_{\text{Ga}} = 1040–1050°\text{C}$).

Such a behavior reminds of the high-temperature SK-growth, where islands are formed after a finite critical thickness. As a matter of fact, the $\Delta a/a$ data always show an increase of the in-plane lattice parameter at the beginning of the growth. At high growth temperatures, this increase is much weaker than at low temperatures. This seems comprehensible, when we suppose that the driving force of platelet formation is low adatom diffusion, which is thermally activated. At high temperature, this should lead, together with a reduced nucleation rate, to rarer islands with larger diameter, i.e., as a whole, with a smaller aspect ratio.

Hence, it seems that the elastic relaxation by islands grown in a SK mode competes with the elastic relaxation by kinetically induced platelets. When the adatom mobility is high due to the presence of a Ga excess[41] and the platelet nucleation rate is small due to low growth rates, the relaxation by platelets is weak and the morphology transition can still be efficient to decrease the elastic energy. When the elastic relaxation by platelets surpasses a critical value, the island morphology transition is no more energetically favorable and will not occur. Under Ga-rich conditions, the buildup of the Ga film will eventually lead to the smoothing of the islands.

This behavior is similar to the case of Si_xGe_{1-x} on Si (Ref. 44) and $In_xGa_{1-x}As$ on GaAs (Ref. 45), where the lattice mismatch is tuned by varying the alloy composition. In both cases, a finite minimum lattice mismatch is necessary to obtain SK growth. An estimation of the minimum lattice mismatch can be deduced from Figs. 12 and 13. In Fig. 12 the slope change due to the quasi-2D–3D transition is clearly visible for $T_{\text{Ga}} = 985–975°\text{C}$. However, it becomes weaker for lower Ga flux and almost disappears at $T_{\text{Ga}} = 970°\text{C}$. In parallel, the relaxation by platelets increases and the residual strain at which the transition occurs decreases. The lattice mismatch still present at the weakest observable slope change for $T_{\text{Ga}} = 970°\text{C}$ can then be tentatively considered as the minimum lattice mismatch. Its value is found to be around $\epsilon = 1.5\%$. Analysis of Fig. 13 gives the same result within experimental precision.

We observe an influence of the elastic relaxation by flat platelets on the 2D–3D transition also at high temperatures. In fact, detailed analysis of Fig. 5 shows that the elastic relaxation due to the roughness of the wetting layer at the 2D–3D transition increases when the Ga flux is decreased. In other words, increasingly N-rich growth conditions lead to rougher wetting layers. To quantitatively assess the critical thickness as a function of growth conditions, GaN growth rates have been previously calibrated to the Ga flux by RHEED intensity oscillations on the same sample. Figure 14 shows that the critical thickness decreases with the amount of residual strain to be relaxed by 3D pyramid formation,

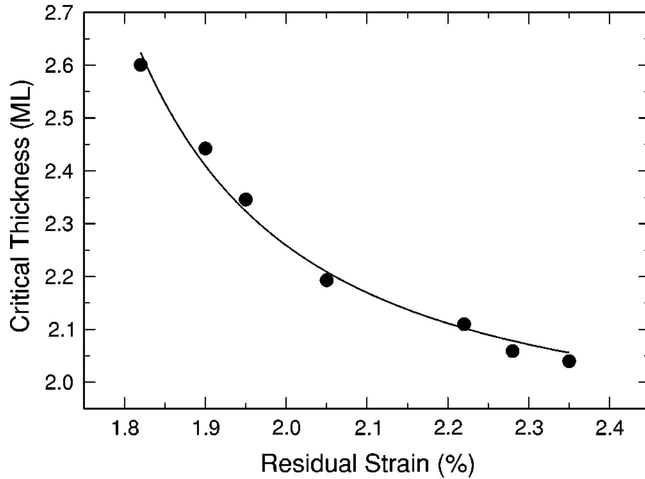

FIG. 14. Critical thickness of GaN islanding as a function of residual strain at the 2D–3D transition for $T_S = 740°C$. Elastic relaxation by platelets on the wetting layer increases the critical thickness, i.e., postpones the 2D–3D transition. The data are deduced from Fig. 5.

i.e., with smoother wetting layers. This residual strain is the difference between the GaN/AlN lattice mismatch (2.4%) and the amount of strain relaxed through platelet formation. Thus, the "driving force" of the 2D–3D transition, i.e., the elastic energy stored in the strained wetting layer, is reduced by the relaxation at the platelets' borders with respect to a fully strained wetting layer and the 2D–3D transition occurs after a larger critical thickness.

A similar effect has been found in the Si_xGe_{1-x}/Si,[44] $In_xGa_{1-x}As/GaAs$,[46] and $In_xAl_{1-x}As/AlAs$ (Ref. 47) systems, where the critical thickness increases with decreasing lattice mismatch. Direct comparison with the present results is, however, difficult, since the strain distribution in the GaN wetting layer should be very inhomogeneous, in contrast to smooth $In_xGa_{1-x}As$ or Si_xGe_{1-x} wetting layers.

VI. GROWTH-MODE PHASE DIAGRAM

The above results can be summarized in a phase diagram that depicts the different modes of elastic relaxation during the first stages of GaN growth on AlN (0001) as a function of the growth parameters. Figure 15(a) shows the summary diagram obtained with a N_2 flow of 0.50 sccm at 300 W rf power, i.e., at maximum growth rates around 0.3 ML/s. The lines are intended as guides to the eye indicating the boundaries between the different growth modes. The symbols represent the measured Ga cell temperatures T_{Ga}, at which the transition between two growth modes occurs, and were extracted from the series of $\Delta a/a$ curves obtained at different substrate temperatures T_S.

First, we see that for all substrate temperatures, a Ga flux exists above which the growth is always 2D. The critical flux increases weakly with temperature, probably due to enhanced Ga reevaporation. Below, we observe a region where transitorily formed islands subsequently coalesce and the growth becomes 2D again and remains so.

For lower Ga fluxes, two regimes exist: at higher temperatures, SK growth is observed, whereas at lower temperatures platelets are formed. At intermediate temperatures ($T_S = 680°C$) SK growth is only possible as a transitory under slightly Ga-rich conditions. Otherwise, the surface diffusion is sufficiently low to produce well-developed platelets that relax elastically and reduce the mismatch sufficiently to suppress the 2D–3D transition.

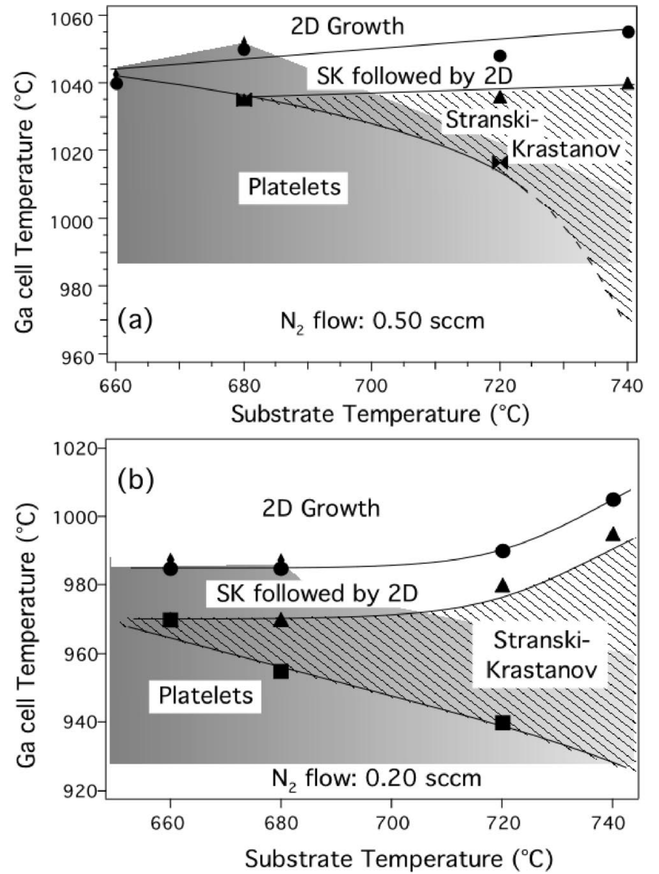

FIG. 15. Growth-mode phase diagram of GaN on AlN at a N_2 flow of (a) 0.50 sccm at 300 W rf power, i.e., at maximum growth rates of 0.3 ML/s and (b) at a N_2 flow of 0.20 sccm at 200 W rf power, i.e., at maximum growth rates of 0.15 ML/s.

The stability region for SK growth increases with increasing substrate temperature. The thermally activated adatom diffusion mobility and the reduced platelet nucleation rate lead to a vanishing roughening of the wetting layer by platelets and consequently to a vanishing elastic relaxation before the 2D–3D transition takes place.

Figure 15(b) shows the phase diagram obtained at lower growth rates with a N_2 flow of 0.20 sccm at 200 W rf power. The main difference to the above case is that the SK growth mode is allowed for lower $T_S = 660°C$, suggesting that the higher mobility due to the lower growth rate suppresses platelet formation and leads to flatter and more strained epilayers.

VII. CONCLUSION

We have shown that for specific Ga fluxes and substrate temperatures, a dynamically stable Ga layer is adsorbed on

(0001) GaN surfaces. The amount of adsorbed Ga is about 2.7 ML in terms of the GaN surface site density, which is in agreement with the Ga bilayer model in Ref. 12 and similar to the results obtained for Ga adsorption on SiC in Ref. 48.

The influence of such a Ga film on the relaxation of GaN layers grown by plasma-assisted molecular-beam epitaxy on AlN(0001) has been studied by *in situ* RHEED measurements of the in-plane lattice parameter variation. Under N-rich conditions, where no Ga accumulates on the surface, an initial elastic relaxation is observed. At high temperatures, this occurs following a Stranski-Krastanov growth mode,[6] whereas at lower temperatures flatter platelets are formed.[10]

Both types of islanding are suppressed under Ga-rich conditions, where a Ga bilayer is expected to form due to accumulation of excess Ga. As a consequence, the growth follows a layer-by-layer Frank-van der Merwe mode. This effect is assigned to a surfactant effect of Ga.

As a matter of fact, it has been previously shown that Ga perfectly wets GaN[12,20] and that it lowers the surface free energy,[12,20] i.e., that it has the tendency to float on the growing surface, two preconditions for surfactant behavior. We propose a microscopic mechanism of the Ga surfactant effect: the first layer of the Ga bilayer coherent to the GaN layer and under strong tensile strain modifies the elastic energy of the epilayer. The elastic relaxation towards larger lattice parameters that is associated with GaN island formation further strains the Ga film and leads to an increase in its elastic energy. Thus, islanding may become energetically unfavorable. Additionally, the adsorbed Ga film increases both Ga and N adatom diffusion[41] and hinders the kinetic formation of platelets, i.e., multilayer growth, at low temperatures.

For slightly Ga-rich conditions, transitory islanding is found, followed by rapid island coalescence. This is due to the finite time required to build up the continuous Ga film on the surface.

We address qualitatively the interaction between SK and platelet growth. In fact, as previously reported, the formation of platelets leads to the elastic relaxation of a significant part of the lattice mismatch at the platelet borders.[10] Albeit, it has to be noted that the driving-force for platelet growth seems not to be the lattice mismatch, but growth kinetics. The low diffusion mobility of the Ga and N adatoms appears to initiate platelet formation by multilayer growth. Nevertheless, this kinetic roughening results in a partial relaxation of the lattice mismatch and thus lowers the elastic energy stored in the initially quasi-2D GaN layer. It is then clear that the appearance of platelets reduces the driving-force for the SK 2D–3D transition, which may be delayed or even suppressed.

From that point of view, the elastic relaxation by islands grown in a SK mode has to compete with the elastic relaxation by kinetically induced platelets. When the relaxation by platelets is sufficiently important, i.e., the residual strain after the critical SK thickness of about 2 ML is lower than about $\epsilon = 1.5\%$, SK growth is impeded. Even when platelets are flat and the elastic relaxation is weak, they still increase the critical thickness of the SK 2D–3D transition. At intermediate temperatures and under slightly Ga rich conditions, a 2D–3D transition takes place even when significant relaxation by platelets occurs.

Systematic measurements of the lattice parameter variation as a function of temperature and Ga flux allow us to outline growth mode diagrams of GaN on AlN(0001) for different growth rates. As a consequence, we are able, by choosing appropriate substrate temperatures and Ga/N ratios, to select whether the growth will be 2D or 3D, i.e., whether we will grow (0001) GaN/AlN quantum well or quantum dot heterostructures.

ACKNOWLEDGMENTS

We would like to thank A. Bourret and J. Brault for useful discussions. Y. Samson is acknowledged for the use of the AFM facility.

[1] For reviews see, e.g., P.M. Petroff and G. Medeiros-Ribeiro, MRS Bull. **21**, 50 (1996); W. Seifert, N. Carlsson, M. Miller, M.E. Pistol, L. Samuelson, and L.R. Wallenberg, Prog. Cryst. Growth Charact. Mater. **33**, 423 (1996); D. Bimberg, M. Grundmann, and N. N. Ledentsov, *Quantum Dot Heterostructures* (Wiley, Chichester, 1999).
[2] L. Goldstein, F. Glas, J.Y. Marzin, M.N. Charasse, and G. Le Roux, Appl. Phys. Lett. **47**, 1099 (1985).
[3] J.M. Moison, F. Houzay, F. Barthe, L. Leprince, E. André, and O. Vatel, Appl. Phys. Lett. **64**, 196 (1994).
[4] D.J. Eaglesham and M. Cerullo, Phys. Rev. Lett. **64**, 1943 (1990).
[5] Y.-W. Mo, D.E. Savage, B.S. Swartzentruber, and M.G. Lagally, Phys. Rev. Lett. **65**, 1020 (1990).
[6] B. Daudin, F. Widmann, G. Feuillet, Y. Samson, M. Arlery, and J.L. Rouvière, Phys. Rev. B **56**, R7069 (1997).
[7] F. Widmann, B. Daudin, G. Feuillet, Y. Samson, J.L. Rouvière, and N.T. Pelekanos, J. Appl. Phys. **83**, 7618 (1998).
[8] B. Damilano, N. Grandjean, F. Semond, J. Massies, and M. Leroux, Appl. Phys. Lett. **75**, 962 (1999).
[9] M. Copel, M.C. Reuter, E. Kaxiras, and R.M. Tromp, Phys. Rev. Lett. **63**, 632 (1989).
[10] A. Bourret, C. Adelmann, B. Daudin, J.-L. Rouvière, G. Feuillet, and G. Mula, Phys. Rev. B **63**, 245307 (2001).
[11] F. Widmann, J. Simon, B. Daudin, G. Feuillet, J.L. Rouvière, N.T. Pelekanos, and G. Fishman, Phys. Rev. B **58**, R15 989 (1998).
[12] J.E. Northrup, J. Neugebauer, R.M. Feenstra, and A.R. Smith, Phys. Rev. B **61**, 9932 (2000).
[13] E.J. Tarsa, B. Heying, X.H. Wu, P. Fini, S.P. DenBaars, and J.S. Speck, J. Appl. Phys. **82**, 5472 (1997).
[14] M. Horn-von Hoegen, B.H. Müller, and A. Al-Falou, Phys. Rev. B **50**, 11 640 (1994).
[15] J. Massies and N. Grandjean, Phys. Rev. Lett. **71**, 1411 (1993).
[16] R. Kern and P. Müller, Surf. Sci. **392**, 103 (1997).
[17] C.W. Snyder, B.G. Orr, and H. Munekata, Appl. Phys. Lett. **62**, 46 (1993).
[18] Y. Robach, A. Solère, M. Gendry, and L. Porte, J. Vac. Sci. Technol. B **16**, 1786 (1998).

[19] R. Leon, C. Lobo, J. Zou, T. Romeo, and D.J.H. Cockayne, Phys. Rev. Lett. **81**, 2486 (1998).
[20] A.R. Smith, R.M. Feenstra, D.W. Greve, M.S. Shin, M. Skowronski, J. Neugebauer, and J.E. Northrup, J. Vac. Sci. Technol. B **16**, 2242 (1998); A.R. Smith, R.M. Feenstra, D.W. Greve, M.S. Shin, M. Skowronski, J. Neugebauer, and J.E. Northrup, Surf. Sci. **423**, 70 (1998).
[21] M. Copel, M.C. Reuter, M. Horn-von Hoegen, and R.M. Tromp, Phys. Rev. B **42**, 11 682 (1990).
[22] D.J. Eaglesham, F.C. Unterwald, and D.C. Jacobson, Phys. Rev. Lett. **70**, 966 (1993).
[23] J.R. Power, K. Hinrichs, S. Peters, K. Haberland, N. Esser, and W. Richter, Phys. Rev. B **62**, 7378 (2000).
[24] J. Massies, N. Grandjean, and V.H. Etgens, Appl. Phys. Lett. **61**, 99 (1992).
[25] N. Grandjean, J. Massies, and V.H. Etgens, Phys. Rev. Lett. **69**, 796 (1992).
[26] H.A. van der Vegt, H.M. van Pinxteren, M. Lohmeier, E. Vlieg, and J.M.C. Thornton, Phys. Rev. Lett. **68**, 3335 (1992).
[27] S. Esch, M. Hohage, T. Michely, and G. Comsa, Phys. Rev. Lett. **72**, 693 (1994).
[28] M. Horn-von Hoegen, F.K. LeGoues, M. Copel, M.C. Reuter, and R.M. Tromp, Phys. Rev. Lett. **67**, 1130 (1991).
[29] D. Kandel and E. Kaxiras, Phys. Rev. Lett. **75**, 2742 (1995).
[30] R.M. Tromp and M.C. Reuter, Phys. Rev. Lett. **68**, 954 (1992).
[31] B.D. Yu and A. Oshiyama, Phys. Rev. Lett. **71**, 585 (1993).
[32] T. Ohno, Phys. Rev. Lett. **73**, 460 (1994).
[33] J. Massies and N. Grandjean, Phys. Rev. B **48**, R8502 (1993).
[34] W.N. Rodrigues, V.H. Etgens, M. Sauvage-Simkin, G. Rossi, F. Sirotti, P. Pinchaux, and F. Rochet, Solid State Commun. **95**, 873 (1995).
[35] N. Grandjean and J. Massies, Phys. Rev. B **53**, R13 231 (1996).
[36] R.H. Miwa, A.C. Ferraz, W.N. Rodriguez, and H. Chacham, Surf. Sci. **415**, 20 (1998).
[37] C.D. Consorte, C.Y. Fong, M.D. Watson, L.H. Yang, and S. Ciraci, Phys. Rev. B **63**, 041301(R) (2001).
[38] H. Chen, R.M. Feenstra, J.E. Northrup, T. Zywietz, J. Neugebauer, and D.W. Greve, J. Vac. Sci. Technol. B **18**, 2284 (2000).
[39] T. Zywietz, J. Neugebauer, M. Scheffler, J.E. Northrup, H. Chen, and R. M. Feenstra (unpublished).
[40] K. Ozasa, Y. Aoyagi, Y.J. Park, and L. Samuelson, Appl. Phys. Lett. **71**, 797 (1997).
[41] T. Zywietz, J. Neugebauer, and M. Scheffler, Appl. Phys. Lett. **73**, 487 (1998).
[42] J. Tersoff, A.W. Denier van der Gon, and R.M. Tromp, Phys. Rev. Lett. **72**, 266 (1994).
[43] C.W. Snyder, J.F. Mansfield, and B.G. Orr, Phys. Rev. B **46**, 9551 (1992).
[44] H.J. Osten, H.P. Zeindl, and E. Bugiel, J. Cryst. Growth **143**, 194 (1994).
[45] K.H. Chang, P.K. Bhattacharya, and R. Gibala, J. Appl. Phys. **66**, 2993 (1989).
[46] N. Grandjean, J. Massies, and F. Raymond, Jpn. J. Appl. Phys. **33**, L1427 (1994).
[47] R. Leon, S. Fafard, D. Leonard, J.L. Merz, and P.M. Petroff, Appl. Phys. Lett. **67**, 521 (1995).
[48] L.X. Zheng, M.H. Xie, and S.Y. Tong, Phys. Rev. B **61**, 4890 (2000).